ELSEVIER

Journal of Photochemistry and Photobiology A: Chemistry 151 (2002) 49–55

Journal of Photochemistry and Photobiology A:Chemistry

www.elsevier.com/locate/jphotochem

Synthesis and characterization of (1″-pyrene butyl)-2-rhodamine ester: a new probe for oxygen measurement in the mitochondria of living cells

A.-C. Ribou*, J. Vigo, J.-M. Salmon

Laboratory of Physico-Chemical Biology of Integrated Systems UPRES 1947, University of Perpignan, 52 Avenue de Villeneuve, F-66860 Perpignan, France

Received 22 March 2002; accepted 8 April 2002

Abstract

For the study of biological system as living cells, access to oxygen concentration in various organelles is of importance. We report here the synthesis, absorption, fluorescence spectra and fluorescence lifetimes of (1″-pyrene butyl)-2-rhodamine ester as a new probe. This compound was designed to target mitochondria. The emission properties have been measured in air-saturated and degassed ethanol solutions at both 340 and 511 nm excitation wavelengths (pyrene and rhodamine centered, respectively). The electronic (emission, excitation) characterizations revealed energy transfer from the pyrene to the rhodamine chromophore. With excitation at 337 nm, the excited state decays biexponentially with a lifetime decay of 0.8 and 30 ns, the latter corresponds to the pyrene chromophore in air-saturated solutions. In degassed solutions the lifetime decay increases up to 220 ns. Those results are used to draw the Stern–Volmer equation. Lifetime measurements in single living cells show that the decay under oxygen atmosphere decrease compared to the one under nitrogen atmosphere.

Keywords: Pyrene; Rhodamine 123; Probe; Lifetime; Intramolecular energy transfer

1. Introduction

There is today evidence that hyperbaric oxygenation of patients greatly improves radiotherapy and chemotherapy [1–3]. However the biological mechanisms leading to the improvement of the effect of cytotoxic drugs is not yet understood; perturbation of the cell cycle [4,5], increase of intracellular free radical production [6–8]. These observations highlight the interest in studying the influence of intracellular oxygen in single living cells on the treatment by cytotoxic drugs such as anthracyclines. Thus it appears important to correlate the intracellular oxygen concentration to the cytotoxic drug effect.

Local oxygen concentrations can be measured in living cells by fluorescence intensity variation [9–12] or fluorescence lifetime changes [13] of pyrene derivatives. Such changes in fluorescence characteristics of pyrene result from dynamic quenching of pyrene by oxygen. Although pyrenebutyric acid or pyrenebutanol are convenient probes for the evaluation of cytosolic oxygen concentrations, they do not allow the measurement of oxygen concentration in mitochondria. These compartments appear to be of great importance since adriamycine cell treatment induces a huge increase in the energetic level of mitochondria [14], which should involve high oxygen consumption. Measurement of mitochondrial O_2 concentration appears necessary which involves the targeting of a pyrene probe. A previous study [15] has shown that Rhodamine 123 (Rh123) linked to long alkyl chains, from C_9 to C_{12}, by an ester bridge, specifically stain mitochondria, as does Rh123. Such results suggested that R123 may be used as a carrier to target heavy fluorescent probes such as pyrene to mitochondria.

We have carried out the synthesis of pyrene derivatives corresponding to the following general formula: R123–alkylchain–pyrene (Fig. 1). We present the synthesis starting from Rh110 and pyrenebutanol (PB) and describe the purification procedure. Preliminary studies of the new probe in ethanol solutions are necessary before studies in the more complex cellular environment are carried out. The absorption, emission fluorescence spectra and fluorescence lifetimes of (1″-pyrene butyl)-2-rhodamine ester (PRE) dye have been measured in air-saturated and degassed ethanol solutions. Comparisons with the reference compounds (Rh123 and PB) are shown and a general behavior presented. Finally we present, for the first time, the lifetime measurements in single living cells.

* Corresponding author. Tel.: +33-4-68-66-21-13; fax: +33-4-68-66-21-44.
E-mail address: ribou@univ-perp.fr (A.-C. Ribou).

1010-6030/02/$ – see front matter © 2002 Published by Elsevier Science B.V.
PII: S1010-6030(02)00152-1

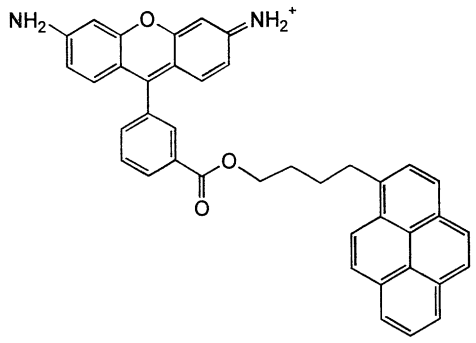

Fig. 1. Structure of PRE.

2. Experimental

2.1. Materials

1-Pyrenebutyric acid (PBA) was purchased from ACROS Organics. Rhodamine 110 chloride and Rh123 chloride were laser grade dyes purchased from Molecular Probe. 1-Pyrenebutanol (PB) was synthesized starting from the acid.

2.2. Synthesis of fluorescent probes

2.2.1. 1-Pyrenebutanol

To 1 g (3.47 mmol) of PBA in dry THF (10 ml) were slowly added 3.8 ml of $LiAlH_4$ (1.0 M solution in diethyl ether). The solution was heated under reflux for 1 h. KOH (1 ml, 1 M) was added and the solution was stirred for a further 15 min. The reaction mixture was filtered on celite. The celite was washed with 300 ml of dichloromethane. Evaporation of the solvents gave the crude product (1 g).

The crude product was purified by chromatography on silica gel using pure dichloromethane as eluant. We obtained a light yellow oily crystal ($R_f = 0.6$, 5% MeOH) as a 70% yield. ^{1}H NMR (400 MHz, DMSO-d6): 1.55 (m, $2H_{CH_2}$); 1.77 (m, $2H_{CH_2}$); 3.28 (q, $J = 7.7$ Hz, $2H_{CH_2}$); 3.43 (q, $J = 5.1$ Hz, $2H_{CH_2}$); 4.31 (t, $J = 5.1$ Hz, $1H_{OH}$); 7.89 (d, $J = 7.9$ Hz, $1H_{pyr}$); 8.00 (t, $J = 7.7$ Hz, $1H_{pyr}$); 8.06 (AB, $J = 9.0$ Hz, $1H_{pyr}$); 8.08 (AB, $J = 9.0$ Hz, $1H_{pyr}$); 8.15 (d, $J = 9.2$ Hz, $1H_{pyr}$); 8.16 (d, $J = 7.9$ Hz, $1H_{pyr}$); 8.20 (dd, $J = 7.7$ Hz, $J = 1.2$ Hz, $1H_{pyr}$); 8.22 (dd, $J = 7.7$ Hz, $J = 1.2$ Hz, $1H_{pyr}$); 8.30 ppm (d, $J = 9.2$ Hz, $1H_{pyr}$).

2.2.2. (1″-Pyrene butyl)-2-rhodamine ester [16]

Rh110 (150 mg, 409 μmol), PB (137 mg, 499 μmol) and 4-dimethylaminopyridine (63 mg, 516 μmol) in dry DMF (3 ml) were mixed under nitrogen. The mixture was gently warmed until the compounds were completely dissolved. DCC (84 mg, 407 μmol) was dissolved in DMF (500 μl) and was added immediately under nitrogen. The reaction, followed by CCM, was left to stir at 100 °C with a $CaCl_2$ trap. After 1 day a further amount of DCC (50 mg) was added. After a further 6 days, acetic acid (0.1 ml) was added and the solution was stirred for 1 h at room temperature. Evaporation of the solvents gave a dark red precipitate. The crude residue was first purified by chromatography on phase transfer (RP8) using a mixture of water/methanol (6:4) as eluant, to remove the Rh110, followed by a mixture water/methanol (2:8). After evaporation of the orange fractions, the pink product was purified by chromatography on silica gel, using dichloromethane as eluant, with increased quantities of methanol (up to 6%). The two purifications by chromatography were carried out a second time. We obtained the pure PRE as a 17% yield. We noticed the presence of dissolved silica, due to the high percentage of methanol employed during the chromatography purification.

^{1}H NMR (400 MHz, DMSO-d6): 1.38 (m, $2H_{CH_2}$); 1.53 (m, $2H_{CH_2}$); 3.17 (m, $2H_{CH_2}$); 3.96 (t, $J = 6$ Hz, $2H_{CH_2}$); 6.82 (s, $1H_{rho}$); 6.83 (s, $1H_{rho}$); 6.84 (d, $J = 8.8$ Hz, $1H_{rho}$); 6.85 (d, $J = 8.8$ Hz, $1H_{rho}$); 6.99 (d, $J = 8.8$ Hz, $2H_{rho}$); 7.49 (dd, $J = 7.4$ Hz, $J = 1.5$ Hz, $1H_{rho}$); 7.78 (td, $J = 7.4$ Hz, $J = 1.5$ Hz, $1H_{rho}$); 7.82 (d, $J = 7.7$ Hz, $1H_{pyr}$); 7.88 (td, $J = 7.4$ Hz, $J = 1.5$ Hz, $1H_{rho}$); 8.07 (t, $J = 7.7$ Hz, $1H_{pyr}$); 8.09 (br s, $4H_{NH_2}$) 8.12 (AB, $J = 9.0$ Hz, $1H_{pyr}$); 8.16 (AB, $J = 9.0$ Hz, $1H_{pyr}$); 8.20 (dd, $J = 7.4$ Hz, $J = 1.5$ Hz, $1H_{rho}$); 8.21 (d, $J = 9.2$ Hz, $1H_{pyr}$); 8.23 (d, $J = 7.6$ Hz, $1H_{pyr}$); 8.25 (d, $J = 9.2$ Hz, $1H_{pyr}$); 8.28 (d, $J = 7.7$ Hz, $1H_{pyr}$); 8.29 ppm (d, $J = 7.7$ Hz, $1H_{pyr}$).

2.3. Equipment and methods

Absorption spectra were taken on a SAFAS 2000 spectrophotometer. Emission fluorescence spectra were recorded using a SAFAS 2000 spectrofluorometer flt. The slit width was 10 nm for both excitation and emission. Relative quantum efficiencies of fluorescence of the three compounds were obtained by comparing the wavelength maximum of the spectrum of the sample in ethanol with that of a solution of Rh123 excited at 511 nm. For spectroscopic measurements, the dye concentration was always kept below 10^{-6} M in order to avoid dye aggregation and reabsorption effects. To check these effects we verified that the Beer–Lambert law remained valid in the concentration range studied.

Cell culture and staining procedure. Experiments were performed on 3T3 mouse fibroblasts (Flow; Cergy Pontoise, France). 3T3 cells were routinely cultured in DMEM supplemented with 2 mM glutamine (ICN, Orsay, France), 10% heat-inactivated fetal calf serum (Gibco, Orsay, France) and the antibiotics penicillin and streptomycin (ICN). Cells were grown in 25 cm^2 flasks at 37 °C in a controlled atmosphere (5% CO_2). For experiments, 3T3 cells were seeded in Sykes–Moore chambers at 30,000–50,000 cells per chamber. After 48 h, the cells were incubated for 30 min in a phosphate saline buffer solution (Hanks') containing 1 μM PRE (1% ethanol). Cells were washed three times and placed in Hanks' balanced salts solution before intracellular fluorescence studies. The stained cells were examined immediately after preparation.

Fluorescence lifetime apparatus. An LSI VSL 337 ND nitrogen laser delivers monochromatic pulses at a wavelength of 337 nm with a full width at half-maximum of 3 ns and a repetition rate adjustable between 1 and 20 Hz. A section of the beam is diffused by ground glass and focused on a photodiode with a rapid response. The signal from the detector is used to provide a timing pulse for triggering the oscilloscope. The light beam is concentrated on the sample either directly when the sample is a solution in a quartz cell or by means of a microscope objective for microscopic samples. Reflecting objective (74×) (Ealing Electro-Optics, Watford, UK) is used to allow excitation of the microscopic sample at a wavelength above 360 nm. The emitted photons are collected and focused on the cathode of a photomultiplier (RCA1P28) which transforms the optical signal into an electrical one. The electrical signal is digitized by a numerical oscilloscope (Tektronix TDS 350) which samples the waveform. The normal sampling rate is 1 gigasample/s. It can be increased with repetitive signals. Normally we carried out 250 successive accumulated signals. To visualize the microscopic field, an SIT camera replaces the photomultiplier; frame grabber (MATROX PULSAR) digitizes the images.

Analysis of the results. The fluorescence response $S(t)$ can be represented as a function of time by the following convolution product $S(t) = G(t) \otimes s(t)$. $G(t)$ represents the apparatus response for the excitation pulse and $s(t)$ the impulse response of the fluorescence. The apparatus response is created with a Gaussian curve convoluted by a time constant. The parameters of the Gaussian and the time constant were obtained after analysis of the response of a solution of POPOP (1,4di-[2-(5-phenyloxazolyl)]-benzene). In most cases, $s(t)$ can be described by the sum of exponentials with time constant τ_i and amplitude A_i. In our experiments we only observed single or double exponential decay. The time constants and amplitude values were obtained by the modulation functions method [17] or by iterative reconvolution using a non-linear least-squares fit [18].

3. Results

3.1. Synthesis of PRE

The crude residue was obtained as described in Section 2. Two-chromatography types were necessary to selectively remove the two starting materials. The chromatography on phase transfer was used to remove Rh110. The chromatography on silica gel to remove PB. Because of the necessity of a very pure compound for fluorescence experiments those chromatographies were carried out a second time. Considering the selectivity of the chromatography on silica gel the presence of pyrene derivatives is excluded. The decomposition possibility was then ruled out since separation in different solvents gave the same spectrum for our compound [19]. In addition PB and PRE mixtures in the proportion 1/100 in different environments (liposome, protein, cell and ethanol) were compared with the spectra of pure PRE and we obtained a different selectivity for each media. Such results make the presence of other compounds extremely unlikely.

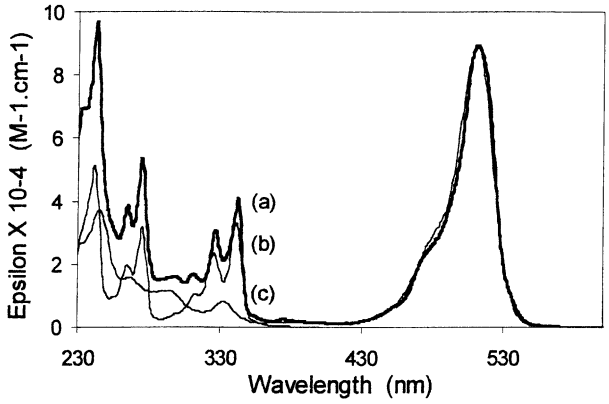

Fig. 2. Absorption spectra represent the variation with wavelength of the molecular extinction coefficient epsilon ($l\,mol^{-1}\,cm^{-1}$) for: (a) PRE (thick line); (b) PB; (c) Rh123 in ethanol, concentration 2×10^{-5} M.

3.2. Absorption

The bichromophoric compound combining both a pyrene group and a rhodamine group is presented in Fig. 1. The chromophores are connected via four methylene groups and an ester group. The PRE absorption spectrum is very similar to a linear combination of PB and Rh123 (Fig. 2). In the pyrene region of the new compound ($\lambda < 400$ nm) the absorption maxima in ethanol are seen at 312, 326 and 341 nm. In the visible region the band of rhodamine shows a maximum at 510 nm in ethanol as does the reference compound. This supports the assumption that rhodamine and pyrene can be regarded as isolated chromophores without any interaction in the fundamental state S_0. The overlap of the rhodamine and pyrene bands in the UV region means that there is no wavelength where pyrene can be selectively excited. For all the fluorescence measurements the compound was therefore excited at a wavelength in the UV region where pyrene absorption is the strongest. However, since rhodamine has fluorescence centered on 530 nm, excitation of rhodamine will not influence the analysis of the emission properties of pyrene.

3.3. Steady-state fluorescence

In ethanol, PRE exhibits a fluorescence spectrum of weaker intensity than that of equal concentrations of Rh123 and PB. We observed a broad band with a maximum at 530 nm, corresponding to the rhodamine chromophore, and a structured band in the UV region corresponding to the pyrene chromophore (Fig. 3). The emission maxima and relative fluorescence intensities are presented in Table 1. The characteristics of the reference compounds are added to allow a comparison. In the visible region, the fluorescence

Table 1
Absorption[a] and fluorescence[b] spectral maxima (in nm) observed for the three compounds in ethanol: PRE, PB and Rh123

System	λ_{max} [ABS] in nm (epsilon in l.mol^{-1} cm^{-1})		λ_{max} [FLUO] in nm (intensity[c])		
			Excitation 340 nm		Excitation 511 nm
Rh123	332 (8200)	510 (92000)	–	530 (2.1)	530 (100)
PBA	312 (11000); 326 (25100); 341 (35400)	–	375 (2.8); 394 (2.5)	–	–
PRE	312 (16800); 326 (31200); 341 (38600)	513 (91500)	375 (0.026); 394 (0.025)	530 (0.26)	530 (8.5)

PRE: (1″-pyrene butyl)-2-rhodamine ester; PB: pyrene butanol; Rh123: rhodamine 123.
[a] Solution of 10^{-5} M in ethanol.
[b] Solution of 10^{-6} M in ethanol.
[c] All intensities are compared to that of Rh123 excited at its emission maximum (511 nm).

spectrum of PRE, obtained for an excitation at 511 nm, shows that the rhodamine fluorescence is quenched compared to the Rh123 reference compound by a factor of 12. The decrease in rhodamine fluorescence is smaller when it is excited at 340 nm. We calculated $R_{511/340}$, the ratio of the intensities of the rhodamine band after excitation at 511 and 340 nm: for PRE $R_{511/340} = 32$ and for Rh123 the ratio increases to 50. Moreover for PRE, in the UV region, the fluorescence intensity of the pyrene band is decreased by a factor of 100 under excitation at 340 nm. These results should indicate an energy transfer from pyrene to rhodamine in PRE, which induces a relative decrease in pyrene fluorescence and a relative increase for rhodamine. To study a possible intermolecular interaction between Rh123 and PB, the fluorescence emission spectra of Rh123 and PB mixture were recorded, increasing the concentration from 10^{-6} to 10^{-4} M. Neither quenching nor energy transfer was detected in these solutions.

3.4. Fluorescence excitation

To get more information on the energy transfer from the pyrene group to the rhodamine group we recorded the fluorescence excitation spectra of PRE and Rh123 observed at 530 nm and of PB observed at 394 nm. The excitation spectra are presented in Fig. 4 between 270 and 450 nm. We observed that the fluorescence excitation spectrum of PRE can be modeled by a linear combination [20] of the excitation spectrum of PB observed at 394 nm and the excitation spectrum of Rh123 observed at 530 nm. These results indicate that, in the fluorescence of the rhodamine group observed at 530 nm, part of the fluorescence is due to an energy transfer from the pyrene group to the rhodamine group. The observations of the fluorescence behavior of the compound as stated above could also be observed in other solvents such as nonanol.

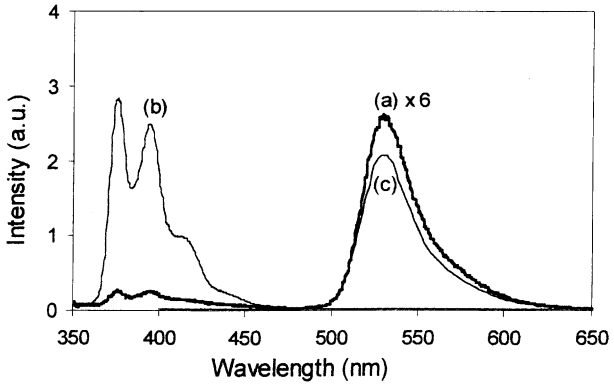

Fig. 3. Emission fluorescence spectra under excitation at 340 nm, expressed in arbitrary units for: (a) PRE (thick line); (b) PB; (c) Rh123 in ethanol at the concentration 1×10^{-6} M. For PRE, the fluorescence spectrum has been multiplied by a factor of 6 for clarity. The relative intensities are calculated by comparison to Rh123 excited at 511 nm (see Table 2).

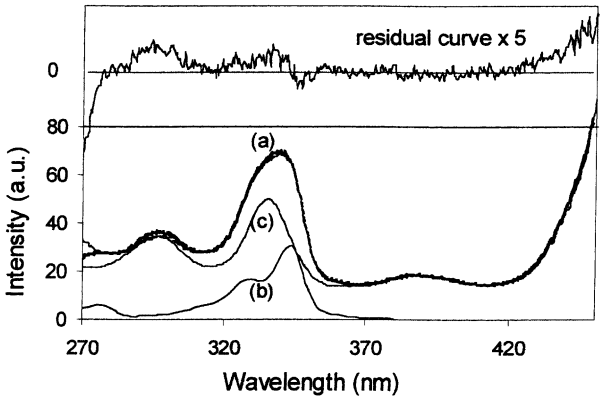

Fig. 4. Excitation spectrum observed at 530 nm in ethanol. At the bottom, the PRE ($C = 1 \times 10^{-6}$ M) experimental fluorescence excitation spectrum, observed at 530 nm, is represented by the thick line (curve a), while the calculated excitation fluorescence spectrum, resulting from the computational resolution of the PRE excitation spectrum into two components PB and Rh123, is represented by the thin line. These curves are nearly superposed. Curves b and c represent the respective calculated participation of PB and Rh123 in the calculated excitation fluorescence spectrum of PRE. At the top, the residual curve (the difference between the experimental and calculated fluorescence excitation spectra of PRE) represents the good fit between the experimental and calculated data.

3.5. Fluorescence decay behavior

The fluorescence decay behavior of PRE has been investigated to obtain further details on the nature of the interaction between the two fluorescent moieties. The fluorescence decays have also been studied both in the absence and presence of oxygen: in oxygen, air and nitrogen-saturated solutions. The 404 and 521 nm filters with a large band pass (∼40 nm)

were used to separate the fluorescence of the pyrene and rhodamine parts. Fig. 5A shows the fluorescence lifetime data obtained with the 521-filter. The steady-state quenching corresponds to the decrease in the rhodamine lifetime in PRE. The lifetime of the rhodamine group is shortened in the presence of the pyrene chain. The fluorescence lifetime of Rh123 in ethanol is 3.6 ns. In the presence of the chain, the lifetime is lowered to 0.8 ns. Fig. 5B shows the time decay profile of the fluorescence of the pyrene group with the 404-filter. These decays show that the lifetimes of PRE and PB in air-saturated solutions are identical. The residual curve confirms the good correlation between the experimental decay and the calculated one. A 2 mV per division curve (inset) reduces the quantification noise for PRE. After degassing with nitrogen (Fig. 5C) we obtained a longer decay curve which gave a fluorescence lifetime of 220 ns, very close to that of PB. No significant difference for these decays is obtained. The fluorescence lifetime of PRE in oxygen saturated ethanol was difficult to obtain due to the quenching of the fluorescence intensity. The iterative reconvolution method gives a fluorescence lifetime of 5.5 ns. With this we reached the limit of detection with the extremely weak intensity of the pyrene band compared to the residual diffusion intensity. For PB a similar value is obtained without difficulty, due to the absence of an energy transfer from pyrene to rhodamine. The decay parameters obtained for the three compounds in ethanol (10^{-6} M) are collected in Table 2.

The preliminary lifetime measurements on PRE loaded single living cell are shown in Fig. 6. The 404 nm band pass filter was used to select the pyrene fluorescence emission. We obtained a double exponential decay when the entire curve was considered. Monoexponential decay gives the same decay value with the later part of the fluorescence decay curve (inset of Fig. 6). The first short live decay is about 6–9 ns and corresponds to the lifetime decay of the cell before staining. It should be considered as the contribution of intracellular NAD(P)H [21]. The fluorescence decays have been studied for cells in control condition, in anaerobiose (N_2 atmosphere) and in hyperoxygenation (O_2 atmosphere). From these fluorescence decays we evaluate lifetime values around: (i) 100 ns for control cells, (ii) 130 ns for cells under N_2, (iii) 65 ns for cell under O_2 atmosphere.

Table 2
Fluorescence decay parameters in ethanol[a] for the three compounds studied in the absence (N_2), in the presence of oxygen (air) and in saturated oxygen solution (O_2): PRE, PB and Rh123

Substance	404 nm filter		521 nm filter	
	Lifetimes (ns) under air	Lifetimes (ns) under N_2	Lifetimes (ns) under O_2	Lifetimes (ns)
Rh123	–	–	–	3.6
PBA	27	216	6	–
PRE	28	220	5.5 ± 2	0.8

PRE: (1″-pyrene butyl)-2-rhodamine ester; PB: pyrene butanol; Rh123: rhodamine 123.

[a] Solution 10^{-6} M in ethanol at room temperature.

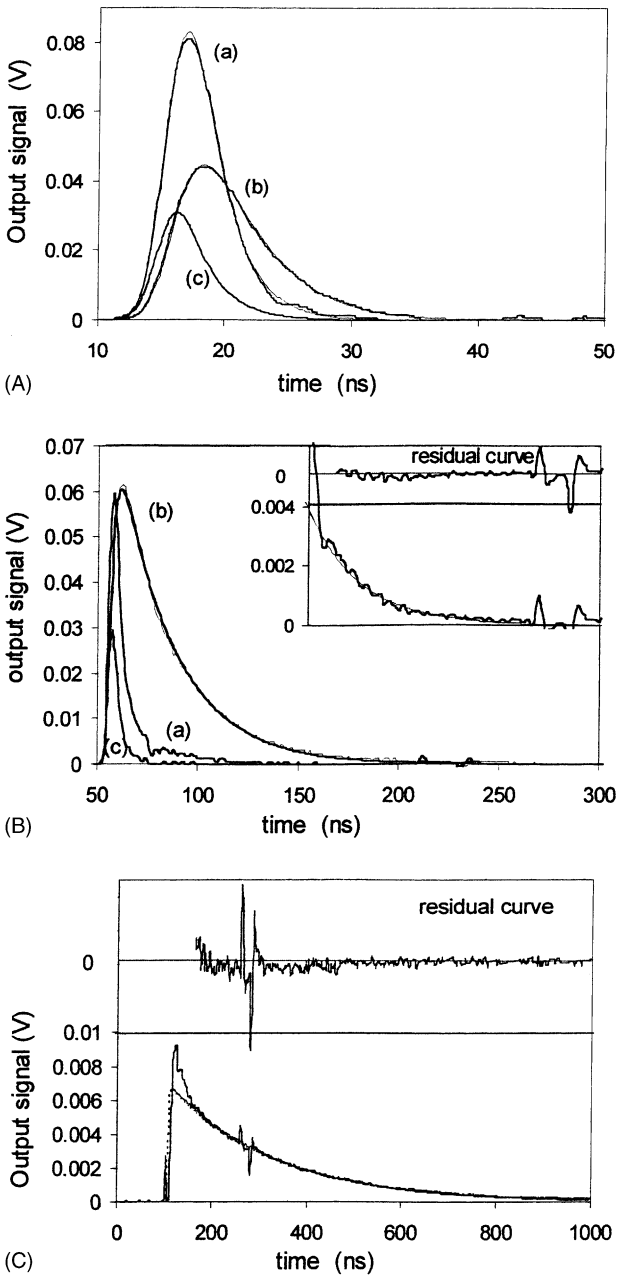

Fig. 5. Fluorescence decay profiles. (A) Emission monitored with the 521 nm bandpath filter. Fluorescence decay curves (thick lines) with their fitting curves (thin lines) of a 1×10^{-6} M aerated ethanol solution after excitation at 337 nm. (a) PRE, (b) Rh123, (c) calculated time-profiles of laser pulse. Fitting curves were calculated by the least-squares method. (B) Emission monitored with the 404 nm bandpath filter. Fluorescence decay curves (thick lines) with their fitting curves (thin lines) of a 1×10^{-6} M aerated ethanol solution after excitation at 337 nm. (a) PRE, (b) PB, (c) laser pulse. Inset: enlargement of the PRE decay profile. The difference between the experimental and calculated curves is shown at the top. (C) Oxygen-free solution of PRE, 404 nm bandpath filter. Fluorescence decay curve (thick solid line) with its fitting curve (dashed line) of a 1×10^{-6} M nitrogen-saturated solution in ethanol after excitation at 337 nm. The difference between the experimental and calculated curves is shown at the top. The fitting curve was calculated by the modulation functions method.

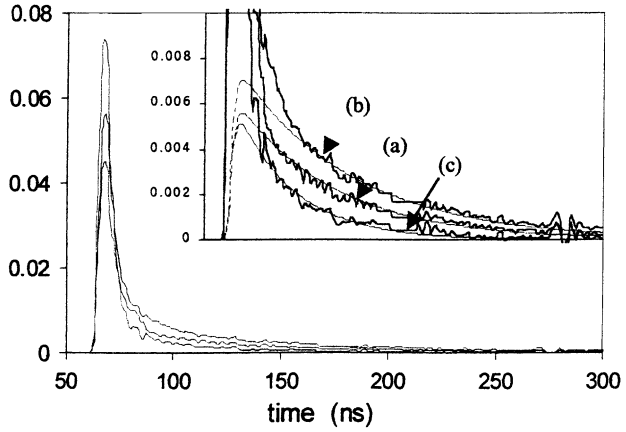

Fig. 6. Fluorescence decay profiles obtained in the same single living cell. 3T3 cells stained with PRE (10 μM) for half-an-hour. (a) Control condition, (b) under nitrogen atmosphere, (c) under oxygen atmosphere. Inset: enlargement of the PRE decay profile. The fitting curves are shown as thin lines.

4. Discussion

4.1. Deactivation pathways

Energy transfer in bichromophoric rhodamine dyes [22] have been studied according to the Förster model. When using rhodamine and diphenyloxazole connected via two methylene groups, Ernsting et al. concluded that an energy transfer, with such a link, is adequately described by the Förster equation model [23]. The exchange mechanism described by Dexter [24] is even further ruled out in our compound due to the four methylene connectors. The deactivation pathway, used to explain the energy transfer for PRE, is based on the energy level scheme presented in Scheme 1. Excitation at 340 nm (open arrow) will excite both the donor

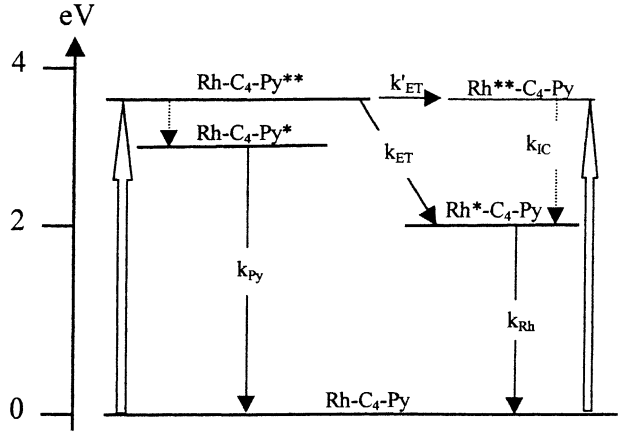

Scheme 1. Simplified deactivation pathways for PRE after excitation in the UV region. Excitation transitions are indicated by open arrows. k_{ET}, k'_{ET}: rates of intramolecular energy transfer to the first and higher excited states of the acceptor rhodamine; k_{IC}: internal conversion rate, k: sum of the deactivation rate constants from the lower excited state including fluorescence.

pyrene and the acceptor rhodamine. Excitation of the rhodamine acceptor into the higher state (noted Rh**–C_4–Py) is followed by fast depopulation to the emitting first excited state (Rh*–C_4–Py). For PRE, radiationless deactivation processes are more efficient than for Rh123 resulting, for the rhodamine group, in a shortened fluorescence lifetime altogether with a decrease in relative fluorescence intensity.

For the pyrene molecule, the Py → Py* ($S_0 \rightarrow S_1$) transitions are weak probability transitions and the molecule is usually efficiently excited via the higher probability $S_0 \rightarrow S_2$ transition [25]. For PRE, emission fluorescence of pyrene occurs from the Rh–C_4–Py* state (S_1) following excitation to the higher state (Rh–C_4–Py**) of the pyrene donor. In competition with this pathway, a Förster energy transfer from the excited pyrene to the rhodamine explains the excitation spectrum shape, when fluorescence was observed at 530 nm, and a decrease in pyrene fluorescence intensity. This is confirmed by the decrease in the ratio $R_{511/340}$, that allows the comparison of the excitation efficiency in the UV region (pyrene + rhodamine) and in the visible region (rhodamine alone) for PRE and Rh123. Furthermore the information obtained from the lifetime decay value is very significant. We do not observe changes in the decay time of the pyrene group in our bichromophoric compound. Such unusual behavior has already been obtained for ruthenium/pyrene compounds [26]. The behavior of our compound is indeed not trivial. But it was already mentioned, in the literature, energy transfer from S_2 [27] in azulene compound. Moreover the pyrene fluorescence from the S_2 state was also detected [28]. We propose a mechanism for the energy transfer described in Scheme 1. Since we do not get changes in the decay time of the pyrene group in PRE compared to PB (28 ns), the energy transfer from pyrene to rhodamine should occur from the Rh–C_4–Py** state (S_2) (Scheme 1, k_{ET} and k'_{ET} constant). This process does not affect the emission from the lower excited state Rh–C_4–Py* (S_1). Thus the emitting process happens from the lower excited state (Rh–C_4–Py*) without a new deactivation pathway and the decay curve shows the same profile as for the reference compound. The effect of oxygen will be studied in the following section.

4.2. Oxygen quantification

In the absence of static quenching, collisional fluorescence quenching is described by the Stern–Volmer equation [29]:

$$\frac{\tau_0}{\tau} = 1 + k_q \tau_0 [O_2]$$

where τ_0 and τ are the excited state lifetimes in the absence and presence of oxygen, respectively, k_q the quenching rate constant and $[O_2]$ the oxygen concentration. Fig. 7 shows the effect of oxygen on PRE and PB lifetimes. The τ_0/τ versus $[O_2]$ dependence was plotted and tested for linearity according to the above equation. This dependence, as shown in Fig. 7, is almost perfectly linear.

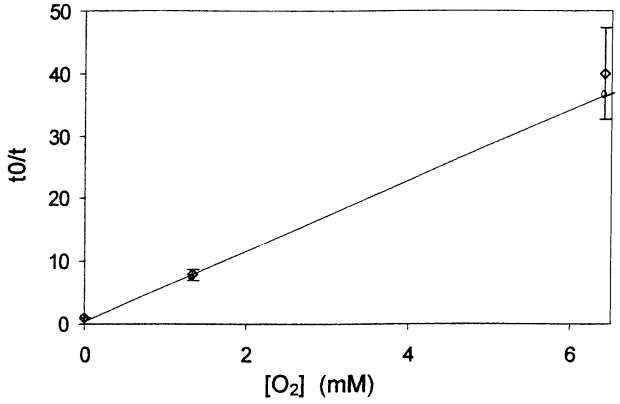

Fig. 7. τ_0/τ versus oxygen concentration. Variation of the decay rate constants ratio with oxygen concentration expressed as a percentage. PRE (◇) and PB (○). The solid line is the best-fit line to the actual data. The slope K_{SV} (Stern–Volmer constant) is 5.6 mmol l^{-1}.

The slope of the Stern–Volmer plot, K_{SV}, in Fig. 7, was found to be 5600 mol l^{-1}. Thus for a τ_0 value of 220 ns, a k_q value of 2.5×10^{10} l mol^{-1} s^{-1} was calculated. This value of the quenching rate constant is in good agreement with the diffusion-controlled rate constant reported for ethanol at 20 °C in the literature [30,31], 9.2×10^9, 5.4×10^9 l mol^{-1} s^{-1}. The long fluorescence lifetime (e.g., 28 ns in aerated ethanol) is the most important feature of pyrene derivatives. It allows the determination of oxygen at relevant concentrations.

4.3. Living cells

The experiment in living cell has been developed elsewhere [19,32]. As a summary we can notice that the localization measurement suggests that PRE is localized in the same intracellular compartments as Rh123, i.e. in mitochondria. Our preliminary results show that the variation range of the lifetime between O_2 and N_2 atmosphere (65 and 130 ns, respectively) is found lower than that observed in solution (Table 2). The lower quenching effect of O_2 could be related to a lower value of the diffusion-controlled rate constant in a membranar environment, while the impossibility to reach under N_2 atmosphere the lifetime obtained in solution may reflect the quenching of PRE by intracellular environment.

5. Conclusion

The newly synthesized compound should enable us to answer the question that interests us: can oxygen concentration be measured in the vicinity of the mitochondria in single living cell? For PRE in solution the lifetime of the pyrene moiety depends on the oxygen concentration. A longer bridge would have decreased even further the Förster energy transfer between pyrene and rhodamine. However our preliminary findings with living cells show that the remaining intensity of the pyrene moiety is high enough to observe its accumulation in mitochondria and obtain a decay curve in situ. The fluorescence lifetime of PRE in living cells is also sensitive to the oxygen concentration. Finally, this energy transfer depends on the environment and therefore should allow us to draw conclusions about this environment. We are currently studying the fluorescence properties of PRE in single living cells and model membranes.

Acknowledgements

This work was supported by the “Ligue Française Contre le Cancer. Comité des P.O.”. The authors thank J. Clifford for carefully reading the manuscript.

References

[1] D.M. Brizel, et al., Cancer Res. 56 (1996) 5347.
[2] M. Nordsmark, M. Overgaard, J. Overgaard, Radiother. Oncol. 41 (1996) 31.
[3] A. Ressel, C. Weiss, T. Feyerabend, Int. J. Radiat. Oncol. Biol. Phys. 49 (2001) 1119.
[4] J.E. Kalns, L. Krock, Anticancer Res. 18 (1998) 363.
[5] J.E. Kalns, E.H. Piepmeier, In Vitro Dev. Biol.—Anim. 35 (1999) 98.
[6] E.W.P. Damen, F.M.H. de Groot, H.W. Scheeren, Expert Opin. Ther. Pat. 11 (2001) 651.
[7] C. Ferraro, et al., Cancer Res. 60 (2000) 1901.
[8] F. Gieseler, M. Clark, K. Stiebeling, M. Puschmann, S. Valsamas, Int. J. Clin. Pharmacol. Ther. 38 (2000) 217.
[9] E. Kohen, J.M. Salmon, C. Kohen, G. Bengtsson, Exp. Cell. Res. 89 (1974) 105.
[10] J.A. Knopp, I.S. Longmuir, Biochem. Biophys. Acta 279 (1972) 393.
[11] D.M. Benson, J.A. Knopp, I.S. Longmuir, Biochim. Biophys. Acta 591 (1980) 187.
[12] E.A. Lissi, T. Caceres, J. Bioenerg. Biomembr. 21 (1989) 375.
[13] D. Huglin, W. Seiffert, H.W. Zimmermann, J. Photochem. Photobiol. B 31 (1995) 145.
[14] E. Rocchi, J. Vigo, P. Viallet, I. Bonnard, J.M. Salmon, Anticancer Res. 20 (2000) 987.
[15] V. Jeannot, Ph.D. Thesis, Perpignan, France, 1996.
[16] J.G. Molotkovsky, Bioorg. Khim. 17 (1991) 976.
[17] B. Valeur, J. Chem. Phys. 80 (1978) 35.
[18] D.V. O’Connor, W.R. Ware, J.C. Andre, J. Phys. Chem. 83 (1979) 1333.
[19] A.-C. Ribou, J. Vigo, P.M. Viallet, J.-M. Salmon, SPIE, in press.
[20] J.-M. Salmon, J. Vigo, P.M. Viallet, Cytometry 9 (1988) 25.
[21] J. Vigo, J.M. Salmon, P. Viallet, Rev. Sci. Instrum. 58 (1987) 1433.
[22] N.P. Ernsting, M. Kaschke, J. Kleinschmidt, K.H. Drexhage, V. Huth, Chem. Phys. 122 (1988) 431.
[23] Th. Förster, Discuss. Faraday Soc. 27 (1959) 7.
[24] D.L. Dexter, J. Chem. Phys. 21 (1953) 836.
[25] D.A. Van Dyke, B.A. Pryor, P.G. Smith, M.R. Topp, J. Chem. Educ. 75 (1998) 615.
[26] J.E. Sohna Sohna, V. Carrier, F. Fages, E. Amouyal, Inorg. Chem. 40 (2001) 6061.
[27] E. Bowen, Luminescence in Chemistry, Van Nostrand, London, 1968.
[28] J.B. Birks, Photophysics of Aromatic Molecules, Wiley, London, 1970.
[29] O. Stern, M. Volmer, Phys. Z. 20 (1919) 183.
[30] S.A. El-Daly, Spectrochim. Acta A 55 (1998) 143.
[31] C.A. Parker, Photoluminescence of Solutions, Elsevier, Amsterdam, 1968.
[32] A.-C. Ribou, J. Vigo, J.-M. Salmon, J. Photochem. Photobiol. B, in preparation.